Chemical Science

ROYAL SOCIETY OF CHEMISTRY

EDGE ARTICLE

View Article Online
View Journal | View Issue

Check for updates

Cite this: *Chem. Sci.*, 2025, **16**, 5036

All publication charges for this article have been paid for by the Royal Society of Chemistry

Received 2nd January 2025
Accepted 18th February 2025

DOI: 10.1039/d5sc00019j

rsc.li/chemical-science

Helix-induced full-color circularly polarized luminescence films with multiple information encryption and multi-stimuli responsiveness†

Shi-Yi Li,[a] Yang Zong,[a] Bing-Hao Liu,[a] Na Liu[b] and Zong-Quan Wu *[a]

The development of full-color circularly polarized luminescence (CPL) materials is of great significance in the field of luminescent materials; however, it is difficult due to the limitations in the synthesis and preparation methods. Helical polymers, with their high optical activity and easy processability, offer a promising solution for the construction of high-performance CPL materials. In this study, we successfully prepared full-color CPL composite films using precisely synthesized polyisocyanide (PI) as chiral source, poly(methyl methacrylate) as the matrix, and commercially available fluorescein as fluorescence source. The introduction of PI not only improves the mechanical properties and fluorescence lifetime of the composite films but also facilitates recyclability through centrifugation after dissolving the composite films with the poor solvent of PI. Moreover, the use of spiropyran as a red fluorescein allows for dynamic responsiveness to light, heat, and acid–base stimuli, broadening the functionality of the CPL materials and constructs a multiple information encryption system. This work presents a low-cost, easily processable, and multi-stimuli responsive strategy for full-color fabrication of CPL materials based on helical PI.

Open Access Article. Published on 18 February 2025. Downloaded on 2/21/2026 7:16:46 PM.
This article is licensed under a Creative Commons Attribution-NonCommercial 3.0 Unported Licence.

Introduction

Helical polyisocyanide (PI) carries a substituent for each carbon atom in its main chain, resulting in an extremely dense structure, and the helical folding of its rigid backbone minimizes the spatial repulsion between the side groups.[1–3] Its helical conformation is stable in both solution and solid states, and the chemical stability enables PI suitable for diverse applications, including optically active materials,[4–6] catalytic materials,[7–9] biotechnology,[10–13] and circularly polarized luminescence (CPL).[14–16] CPL has special polarization properties and carries spin angular momentum, which has important applications in optoelectronic devices,[17,18] smart sensing,[19,20] 3D displays,[21] information encryption, and anti-counterfeiting.[22,23] In particular, multiple information encryption and anti-counterfeiting can be realized by using CPL materials. So far, various chiral luminescent systems have been developed, including metal complexes,[24–26] organic small molecules,[27,28] polymers,[29–31] supramolecular systems,[32–34] and liquid crystals.[35–37] Among these, helical polymers stand out due to their high stability, processability, and unique helical chirality, which make them ideal for designing high-performance CPL materials. However, there is relatively limited research on CPL materials based on helical PI.

Conventional solution-based luminescent systems are usually limited by the solubility, toxicity, and evaporation of organic solvents, as well as by the application scenarios. In contrast, composite films can be used in a variety of applications by adjusting their composition.[38–42] In addition, composite films possess a certain mechanical strength to maintain stability under high pressure or harsh environments, and can be processed into diverse shapes and sizes using techniques such as coating, laminating, and injection molding to adapt to different application requirements. Composite films usually have a long service life, thereby reducing the costs of replacement and maintenance. Additionally, their production and usage generally have a minimal environmental impact, aligning well with the requirements of sustainable development. Composite films also demonstrate good recyclability, reducing the generation of waste. In summary, composite films possess significant advantages in terms of structural stability, processability, cost-effectiveness, and environmental friendliness, making them an excellent choice for the preparation of luminescent materials. Moreover, white light-emitting devices based on organic molecules have received great attention in the field of optoelectronics.[43–45] For composite films, white light-emitting films can be easily prepared using a simple mixture of three-color fluorescein.

[a]*State Key Laboratory of Supramolecular Structure and Materials, College of Chemistry, Jilin University, Changchun 130012, China. E-mail: zqwu@jlu.edu.cn*

[b]*The School of Pharmaceutical Sciences, Jilin University, 1266 Fujin Road, Changchun, Jilin, 130021, P. R. China*

† Electronic supplementary information (ESI) available: Detailed experimental process and additional data associated with this work. See DOI: https://doi.org/10.1039/d5sc00019j

© 2025 The Author(s). Published by the Royal Society of Chemistry

Open Access Article. Published on 18 February 2025. Downloaded on 2/21/2026 7:16:46 PM.
This article is licensed under a Creative Commons Attribution-NonCommercial 3.0 Unported Licence.

Multi-stimuli responsive CPL materials are smart materials with multiple stimulus-responsive properties, combining the uniqueness of CPL with the flexibility of multi-stimuli responsiveness.[46–49] These materials can respond to multiple external stimuli, such as light, heat, and chemicals, enabling multifunctional integration, stable performance, and versatile functionality in complex and dynamic environments. In addition, these materials can respond quickly and significantly to external stimuli, allowing precise control over their luminescent and circular polarization properties by adjusting the intensity and type of stimuli. In information encryption and anti-counterfeiting technology, multi-stimuli responsiveness combined with CPL can improve the anti-counterfeiting ability and identification accuracy of the material.[50,51]

In this work, we utilized chiral helical PI as a chiral source, commercially available nile red (red), coumarin 6 (green), and 1-(4-carboxyphenyl)-1,2,2-triphenylethene (blue) as fluorescence sources, and poly(methyl methacrylate) (PMMA) as matrix material (Scheme 1a). A variety of full-color CPL composite films with different emission wavelengths were successfully prepared. It is noteworthy that white CPL materials can be easily constructed by controlling the mixing ratio of the three small molecule fluoresceins. The introduction of PI not only improves the fluorescence lifetime and mechanical properties of the composite films but also facilitates patterning. Helical PI can be recycled by centrifugation after dissolving the composite film with the poor solvent of PI, thereby reducing the production cost of the material and promoting practical production applications. Furthermore, by incorporating spiropyran (SP) as a red fluorescent unit, we prepared CPL composite films that are dynamically responsive to UV light, heat, and acid–base stimuli. Patterned erasure, dynamic color response, and multi-stimuli responsive CPL of composite films can be achieved and a multiple information encryption system has been successfully constructed.

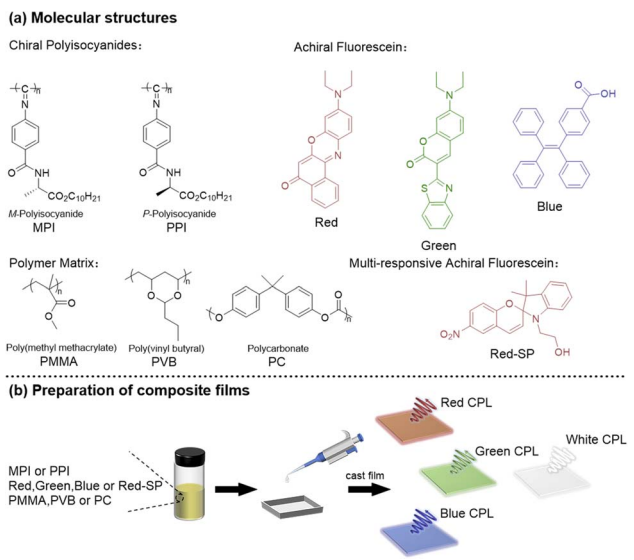

Scheme 1 (a) Molecular structures of chiral helical PI, achiral fluorescein, multi-responsive achiral fluorescein, and polymer matrix. (b) Scheme of the preparation of composite films.

Results and discussion

Left- and right-handed helical polyisocyanide (M-PI and P-PI) with a polymerization degree of 100 were prepared according to previous research.[52] The composite films were obtained by pouring a chloroform solution containing matrix, polymer, and fluorescein into a polytetrafluoroethylene (PTFE) mold and allowing the solvent to evaporate at room temperature (Scheme 1b). Details regarding dosage and procedure are provided in ESI.† In order to exclude the effect of linear polarization of the prepared composite films, the circular dichroism (CD) and UV-vis absorption spectra of the PI-PMMA composite film were tested by rotating the film at different angles relative to the optical axis (Fig. S1†). The consistent CD signals indicated negligible contributions from linear polarization and birefringence. In addition, we screened the addition amount of PI and fluorescein (Fig. S2†). When the content of PI and fluorescein was high, the light transmittance of the composite film was seriously decreased, limiting their practical use. For display applications utilizing RGB color system, achiral fluorescein with red, green, and blue emissions was introduced into the composite films to create PI-R-PMMA, PI-G-PMMA, and PI-B-PMMA, respectively. These films all exhibited UV absorption at 250–700 nm, with the absorption at 250–600 nm attributed to PI and fluorescein, and the absorption at 600–700 nm to light scattering (Fig. 1a and b). In addition, the composite films exhibited CD signals at 250–700 nm, and their positions were almost identical to those of PI-PMMA films. In the UV absorption spectrum, strong absorption from red fluorescein was observed at 500–600 nm, but no corresponding CD was observed, suggesting fluorescein lacked induced chirality. The strong cotton effect at 250–500 nm originated from the chiral PI, and the CD at 500–700 nm was attributed to circularly polarized scattering. Under UV light (365 nm) excitation, the PI-R-PMMA, PI-G-PMMA, and PI-B-PMMA displayed obvious red, green, and blue emissions, with the maximum emission peaks located at 630 nm, 511 nm, and 486 nm, respectively (Fig. 1c).

The chiral fluorescent composite films were characterized by CPL. In the wavelength range of 400–750 nm, PI-R-PMMA, PI-G-PMMA, and PI-B-PMMA all showed obvious mirror-image CPL signals, indicating the successful preparation of full-color CPL-active thin films (Fig. 2a). Their maximum asymmetry factors (g_{lum}) were 1.3×10^{-3} (red), 5.5×10^{-3} (green), and 5.7×10^{-3} (blue) (Fig. S3a†). In addition, the fluorescein used in this work contained both aggregation-induced quenching (ACQ) and aggregation-induced emission (AIE) molecules, which further demonstrated the universality of this system for the preparation of CPL-active materials. The composite film (PI-R/G/B-PMMA) with white fluorescence emission (Fig. 2b and d) and white CPL (Fig. 2c) could be obtained by modulating the mixing ratio of the three fluorescein. To expand the range of applications for these CPL composite films, poly(vinyl butyral) (PVB) and polycarbonate (PC) were also selected as matrix materials for the composite films, alongside PMMA. PVB is known for its flexibility and impact resistance, while PC offers good transparency and excellent electrical insulation, making it widely used in the

Open Access Article. Published on 18 February 2025. Downloaded on 2/21/2026 7:16:46 PM.
This article is licensed under a Creative Commons Attribution-NonCommercial 3.0 Unported Licence.

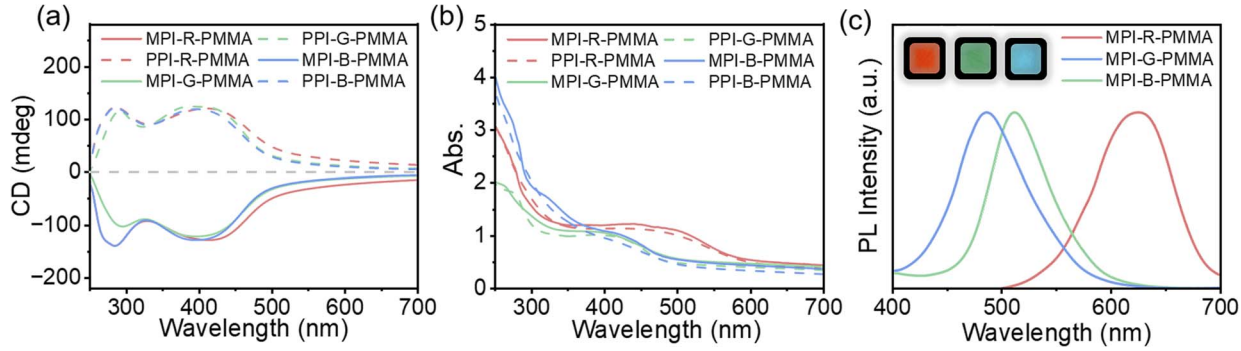

Fig. 1 CD (a) and UV-vis (b) spectra of the chiral fluorescence composite films. (c) PL spectra and luminescence photographs of the chiral fluorescence composite films.

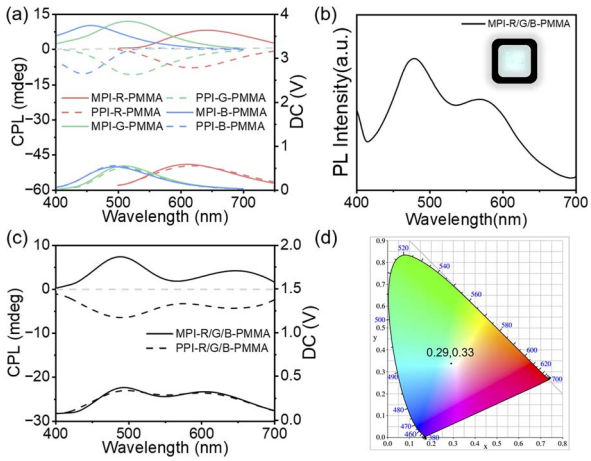

Fig. 2 (a) CPL spectra of chiral fluorescence composite films. (b) PL spectra of white MPI-R/G/B-PMMA composite film. (c) PL spectra of chiral white fluorescence composite film. (d) Chromaticity coordinates of white chiral white fluorescence composite film.

electronic industry. Composite films with RGB emission were prepared by replacing the PMMA with PVB or PC (PI-R-PVB, PI-G-PVB, PI-B-PVB, PI-R-PC, PI-G-PC, and PI-B-PC) using the above method. The PVB composite films showed CD signals similar to those of PMMA composite films (Fig. S4a–c†). However, the PC composite films showed a specific CD signal, probably due to the interaction between the PI and the benzene structure in the PC. (Fig. S5a–c†). Both PVB and PC composite films demonstrated significant RGB emission under 365 nm UV excitation significant RGB emission was shown under 365 nm UV excitation (Fig. S4d–f and S5d–f†). In addition, all composite films showed clear mirror-image CPL signals (Fig. S6 and S7†), their glum values of the PVB and PC based composite films were similar to those prepared with PMMA. The glum values were 1.5 $\times$ 10^{-3} (red), 5.5 $\times$ 10^{-3} (green), and 6.3 $\times$ 10^{-3} (blue) for PVB based composite films; and were 0.9 $\times$ 10^{-3} (red), 4.3 $\times$ 10^{-3} (green), and 3.6 $\times$ 10^{-3} (blue) for PC based composite films (Fig. S3b and c†) indicating the generalizability of this preparation method. We also found that polymer matrix (PMMA, PC, and PVB) exhibited no fluorescence, CD, and CPL signals (Fig. S8a, S9a, and S10a†); composite films containing only chiral PI (PMMA-PI, PVB-PI, and PC-PI) had CD signals but no fluorescence and CPL signals; and composite films containing only achiral fluorescein (PMMA-R, PMMA-G, PMMA-B, PVB-R, PVB-G, PVB-B, PC-R, PC-G, and PC-B) had fluorescence signals but no CD and CPL signals (Fig. S8–S10†). Therefore, the combination of chiral PI and achiral fluorescein was essential for the preparation of composite films with CPL properties, demonstrating the necessity of this method.

It has been demonstrated that composite films using polyacetylene as the chiral source can selectively absorb fluorescence with different spins to produce CPL emission by the single-handed excess helical structure of chiral helical polyacetylene even without any interaction between the chiral and fluorescent units.[53] In order to investigate whether a similar property existed in the composite films with PI as the chiral source, we further conducted side-by-side CPL tests of chiral PI composite film (PI-PMMA) and nonchiral fluorophore film (R-PMMA, G-PMMA, and B-PMMA). When the excitation light first passed through R-PMMA, G-PMMA, or B-PMMA and then through PI-PMMA, the CPL signals were detected in both green and blue emitting regions of the stacked films, with the signals opposite in direction to the CD signals. This result was consistent with the matching rule (Fig. 3a and c). In previous study, the CPL signal was not detected because the red emission region (550–650 nm) did not overlap with the CD spectrum of polyacetylene, violating the matching rule.[53,54] Interestingly, in this study, we detected CPL signals in the red emission region. We found that PI-PMMA retained some CD signals at 500–700 nm, which are attributed to circularly polarized scattering effect caused by the aggregation of rigid PI in the film.[55] Therefore, the red emission region (550–650 nm) was still suitable for the CPL selective absorption mechanism based on the matching rule to generate CPL signals. It was worth noting that the CPL selective absorption mechanism produced a high intensity CPL signal with g_{lum} of 1.8 $\times$ 10^{-2}.

In previous research, due to the selective absorption mechanism of the matching rule, the CPL signal was not detected when the excitation light passed through PI-PMMA first and then through R-PMMA, G-PMMA, or B-PMMA.[53,54] Surprisingly, CPL signals were detected in the red, green, and blue emission regions when the excitation light passed through PI-PMMA first

© 2025 The Author(s). Published by the Royal Society of Chemistry

Open Access Article. Published on 18 February 2025. Downloaded on 2/21/2026 7:16:46 PM.
This article is licensed under a Creative Commons Attribution-NonCommercial 3.0 Unported Licence.

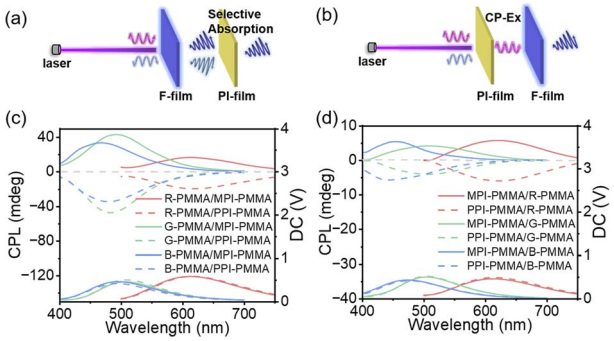

Fig. 3 (a and c) Scheme of CPL generation mechanism and CPL spectra when the excitation light passed through R-PMMA, G-PMMA or B-PMMA first and then PI-PMMA. (b and d) Scheme of CPL generation mechanism and CPL spectra when the excitation light passed through PI-PMMA first and then R-PMMA, G-PMMA or B-PMMA.

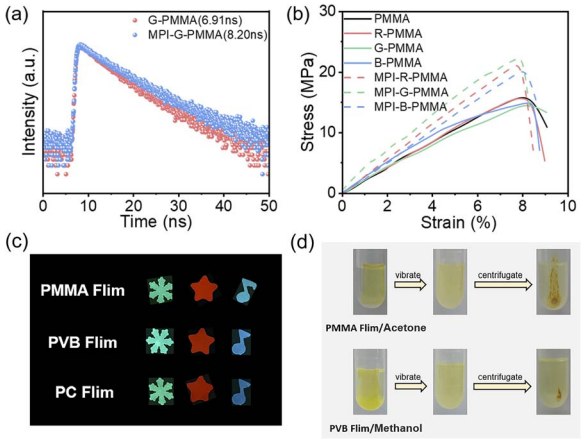

Fig. 4 (a) The phosphorescence decay curves at room temperature of the G-PMMA and MPI-G-PMMA. (b) Stress–strain curves of the PMMA composite film. (c) Fluorescence photographs of patterned composite films. (d) Scheme of polymer recycling.

and then through R-PMMA, G-PMMA, or B-PMMA (Fig. 3d). We speculated that this resulted from the circularly polarized light excitation (CP-Ex) mechanism,[56] where non-polarized excitation light source was partially absorbed by the rigid PI composite film, converting it into a polarized light source, which excited the non-chiral fluorophore film to produce CPL (Fig. 3b). We also performed the same tests on composite films based on PVB and PC, both of which were able to detect full-color CPL signals in stacking orders (Fig. S11 and S12†). The CPL intensity of the composite film was found to be between the intensities produced by the CP-Ex mechanism and the CPL selective absorption mechanism. Therefore, we concluded that the CPL generation mechanism of the composite film may originate from the synergistic action of the two mechanisms. The generation of CPL in composite films made of different materials follows the similar mechanism, and the substrate materials have no significant influence onto the CPL, so their g_{lum} are almost the same. In summary, PI materials are one of the excellent choices for constructing CPL materials.

Due to the domain-limiting effects of PI on fluorescein in the films, the PMMA, PVB, and PC composite films prepared with fluorescein all showed a small increase in fluorescence lifetime (up to 18%) after the introduction of PI (Fig. 4a and S13†). PI is a stable rigid helical structure; for three different matrix composite film materials, it can achieve a small reduction in film elongation at break (maximum 9.4%) while significantly increasing the tensile strength of the composite film (maximum 98.8%) (Fig. 4b and S14†). In addition, the composite film exhibited excellent plasticity, enabling a wide range of patterning using different patterned molds (Fig. 4c). Since PI is poorly soluble in acetone and methanol, while PMMA can be dissolved in acetone and PVB can be dissolved in methanol, and fluorescein is soluble in both acetone and methanol, PI can be recovered and reused by centrifugation based on the difference in solubility (Fig. 4d). In summary, the composite films using PI as a chiral source, nonchiral fluorescein as a fluorescence source, and PMMA, PVB, or PC as matrices were characterized by low cost, processability, and high intensity, and have great potential application value in the field of CPL display materials.

Dynamic display has been a key focus in the field of luminescent display. In this work, we replaced the red fluorescein with SP which has dynamic response properties. Then, we prepared composite films (PI-SP-PMMA) using PMMA as the matrix and PI as the chiral source. As the UV irradiation time (365 nm) increased, the UV absorption curve of PI-SP-PMMA gradually showed the characteristic absorption peaks associated with the SP ring-open (560 nm) (Fig. S15a†). Meanwhile, the CD curve of PI-SP-PMMA remained unchanged with the prolonged light exposure (Fig. S15b†). Subsequently, blue and green fluorescein (PI-SP*x*G*x*-PMMA and PI-SP*x*R*x*-PMMA, *x* represents the mass of fluorescein in mg) were reintroduced into the composite films. The fluorescent color of the films changed continuously with the increasing light irradiation time. There was a gradual transition from green or blue fluorescence to mixed-color fluorescence with red. By adjusting the ratio of the two fluorescein, a dynamic display system with multiple colors can be constructed (Fig. 5a and c). Due to the limitation in the testing method, we examined the fluorescence and CPL of the films after 10 s of UV light irradiation. Different fluorescein ratios produced different fluorescence colors and CPL signals (Fig. S16† and 5b, d). As the amount of green or blue fluorescein increased, the luminescence color gradually shifted from red to light purple and light pink. It can be inferred that the CPL curves of the films changed continuously throughout the light irradiation.

In addition, due to the dynamic responsiveness of the SP, the patterned writing can be performed using a mold under light illumination, followed by ring-closing of the SP under visible light irradiation or heating (40 °C), and erasure of the pattern. Multiple writing and erasing of information can be realized. This feature facilitated the sequential inscription and removal of different 2D code patterns (*e.g.*, J, L, U, and CC) on the same composite film (Fig. 6a). The UV-absorption intensity at 560 nm, measured before and after erasure using visible light irradiation

Open Access Article. Published on 18 February 2025. Downloaded on 2/21/2026 7:16:46 PM.
This article is licensed under a Creative Commons Attribution-NonCommercial 3.0 Unported Licence.

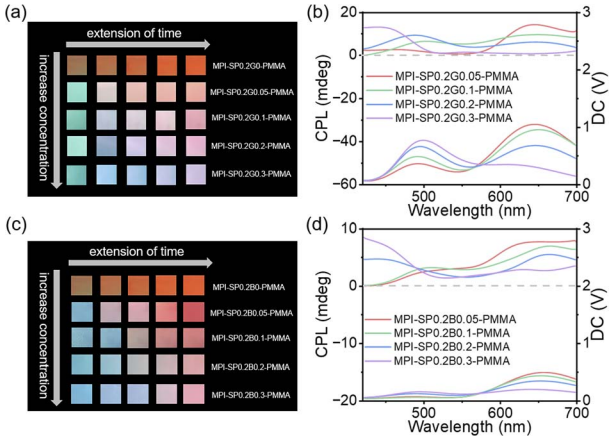

Fig. 5 Luminescence photographs of chiral fluorescence composite film (a) with different SP and green fluorescein ratios or (c) with different SP and red fluorescein ratios. CPL spectra of chiral fluorescence composite film (b) with different SP and green fluorescein ratios or (d) with different SP and red fluorescein ratios.

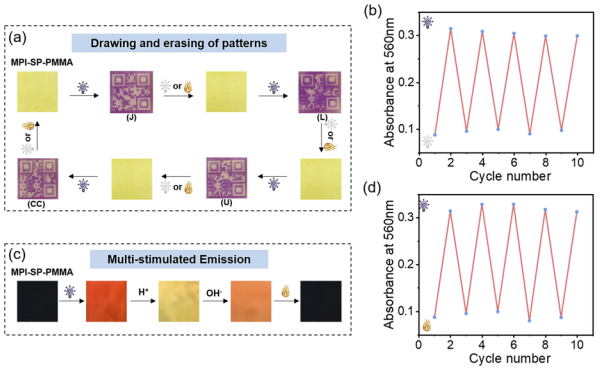

Fig. 6 (a) Scheme of pattern erasure on MPI-SP-PMMA composite film. (b and d) Erasure cycle curve of UV absorption intensity at 560 nm for MPI-SP-PMMA composite film. (c) Scheme of multi-stimulated emission of MPI-SP-PMMA composite film.

or heating, demonstrated excellent erasure cycle characteristics (Fig. 6b and d). In addition to photo-thermal response, SP was also responsive to acids and basic conditions. After 10 s of UV irradiation, the composite film exhibited red fluorescence. Immersion in aqueous acetic acid (PH = 2.4) for 10 s changed the fluorescence color to yellow, while exposure to ammonia (PH = 12.9) for 10 s restored the red fluorescence color. Heating then returned the SP to its ring-off state (Fig. 6c). In addition to the change in fluorescence spectrum, its CPL spectrum and g_{lum} also changed (Fig. S17†). The maximum g_{lum} changed from 1.5 $\times 10^{-3}$ (PH = 2.4) to 0.8 $\times 10^{-3}$ (PH = 12.7).

The unique multicolor CPL properties of the composite film made it suitable for applications in multiple message encryption. A mixed solution containing PMMA, PI, and fluorescein, used in the preparation of the composite film, was employed as the ink to write the numbers 1–9 on a glass plate as the initial message (Fig. 7). Under sunlight, the sequence "726382915" can be identified. The ink with SP as fluorescein was added and the color changed from light yellow to red after 10 s of exposure to

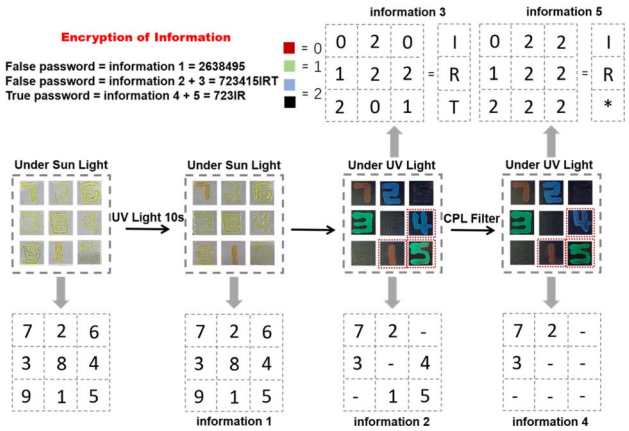

Fig. 7 PMMA solution containing SP and helical PI was utilized as ink for writing on a glass plate with the numbers 1–9. Information encryption was achieved using UV light and CPL filter.

UV light. The first incorrect password information 1 "2638495" was identified. Under the UV light, the fluorescein-containing ink showed fluorescence, which can identify the information 2 "723451". Different fluorescent colors were assigned to the logical information: red for 0, green for 1, blue and black for 2. Based on the customized codebook (Table S1†), the information 3 "IRT" was decoded, producing a second incorrect code "723451IRT". Using L-circular polarization filter, we can get information 4 "723". Combining this with the color and the codebook, information 5 'IR' was obtained, ultimately revealing the correct password "723IR".

Conclusions

In summary, we have successfully prepared full-color CPL composite films using helical PI as chiral source, PMMA as matrix, and commercially fluorescein as fluorescence source. White CPL materials were prepared by adjusting the mixing ratio of the three fluorescein. The composite films also exhibited excellent processability and can be patterned. The introduction of PI enhanced the tensile strength and the fluorescence lifetime of the composite films, and the helical PI can be recovered by solvent centrifugation. These results demonstrated the versatility of the method for preparing CPL composite films based on helical PI, demonstrating excellent mechanical and optical properties, as well as the potential for low-cost recycling. It had excellent potential for development in practical production applications. Additionally, the inclusion of SP as a red fluorescein enriched the optical properties, producing CPL materials with multicolor light response and acid–base response properties and a multiple information encryption system was successfully constructed. This further demonstrated that helical PI was an excellent choice for the fabrication of high-performance CPL materials.

Data availability

The data supporting this article have been included as part of the ESI.†

© 2025 The Author(s). Published by the Royal Society of Chemistry

Open Access Article. Published on 18 February 2025. Downloaded on 2/21/2026 7:16:46 PM. This article is licensed under a Creative Commons Attribution-NonCommercial 3.0 Unported Licence.

Author contributions

Z.-Q. W. and N. L. designed and directed the project, S.-Y. L. and B.-H. L. performed the experiments and analyzed the data. Z.-Q. W., S.-Y. L., and Z. Y. wrote the manuscript with input from all other authors.

Conflicts of interest

There are no conflicts to declare.

Acknowledgements

Financial supports from National Natural Science Foundation of China (NSFC, grants no. 92256201, 52273006, 92356302, 22071041, and 21971052) and Natural Science Foundation of Jilin Province (20240101181JC) are gratefully appreciated.

Notes and references

1 C. Kollmar and R. Hoffmann, *J. Am. Chem. Soc.*, 1990, **112**, 8230–8238.
2 N. Liu, L. Zhou and Z.-Q. Wu, *Acc. Chem. Res.*, 2021, **54**, 3953–3967.
3 R. Deng, C. Wang and M. Weck, *ACS Macro Lett.*, 2022, **11**, 336–341.
4 T. Kajitani, H. Onouchi, S.-i. Sakurai, K. Nagai, K. Okoshi, K. Onitsuka and E. Yashima, *J. Am. Chem. Soc.*, 2011, **133**, 9156–9159.
5 C. Wang, R. Deng and M. Weck, *Macromolecules*, 2023, **56**, 3507–3516.
6 N. Kanbayashi, S. Tokuhara, T. Sekine, Y. Kataoka, T.-a. Okamura and K. Onitsuka, *J. Polym. Sci., Part A: Polym. Chem.*, 2018, **56**, 496–504.
7 K. Kishi, T. Ishimaru, M. Ozono, I. Tomita and T. Endo, *Polym. J.*, 2000, **32**, 294–296.
8 T. Miyabe, Y. Hase, H. Iida, K. Maeda and E. Yashima, *Chirality*, 2009, **21**, 44–50.
9 X.-H. Xu, R.-T. Gao, S.-Y. Li, L. Zhou, N. Liu and Z.-Q. Wu, *Chem. Sci.*, 2024, **15**, 12480–12487.
10 J. Kumari, O. Paul, L. Verdellen, B. Berking, W. Chen, L. Gerrits, J. Postma, F. A. D. T. G. Wagener and P. H. J. Kouwer, *ACS Appl. Bio Mater.*, 2024, **7**, 3258–3270.
11 A. N. Gudde, M. J. J. van Velthoven, P. H. J. Kouwer, J.-P. W. R. Roovers and Z. Guler, *Biomaterials*, 2023, **302**, 122337.
12 R. Sun, X. Jin, Y. Bao, Z. Cao, D. Gao, R. Zhang, L. Qiu, H. Yuan and C. Xing, *Nano Lett.*, 2024, **24**, 3257–3266.
13 M. J. J. van Velthoven, A. N. Gudde, M. van der Kruit, M. P. C. van Loon, L. Rasing, F. A. D. T. G. Wagener, J.-P. Roovers, Z. Guler and P. H. J. Kouwer, *Adv. Healthcare Mater.*, 2024, **13**, 2302905.
14 T. Ikai, M. Okubo and Y. Wada, *J. Am. Chem. Soc.*, 2020, **142**, 3254–3261.
15 T. Jiang, Y. Zhang, L. Hua, H. Li, J. Zhao, S. Yan and Z. Ren, *Mater. Sci. Eng., R*, 2024, **160**, 100818.
16 N. Liu, R.-T. Gao and Z.-Q. Wu, *Acc. Chem. Res.*, 2023, **56**, 2954–2967.
17 Z. Geng, Y. Zhang, Y. Zhang, Y. Quan and Y. Cheng, *Angew. Chem., Int. Ed.*, 2022, **61**, e202202718.
18 J.-M. Teng and C.-F. Chen, *Adv. Opt. Mater.*, 2023, **11**, 2300550.
19 S. Wang, D. Hu, X. Guan, S. Cai, G. Shi, Z. Shuai, J. Zhang, Q. Peng and X. Wan, *Angew. Chem., Int. Ed.*, 2021, **60**, 21918–21926.
20 S. Wang, S. Xie, H. Zeng, H. Du, J. Zhang and X. Wan, *Angew. Chem., Int. Ed.*, 2022, **61**, e202202268.
21 L. E. MacKenzie and R. Pal, *Nat. Rev. Chem.*, 2021, **5**, 109–124.
22 Z. Huang, Z. He, B. Ding, H. Tian and X. Ma, *Nat. Commun.*, 2022, **13**, 7841.
23 K. Fu, D.-H. Qu and G. Liu, *J. Am. Chem. Soc.*, 2024, **146**, 33832–33844.
24 Z.-L. Gong, Z.-Q. Li and Y.-W. Zhong, *Aggregate*, 2022, **3**, e177.
25 J. Song, H. Xiao, L. Fang, L. Qu, X. Zhou, Z.-X. Xu, C. Yang and H. Xiang, *J. Am. Chem. Soc.*, 2022, **144**, 2233–2244.
26 D.-H. Kong, Y. Wu, C.-M. Shi, H. Zeng, L.-J. Xu and Z.-N. Chen, *Chem. Sci.*, 2024, **15**, 16698–16704.
27 Z.-L. Gong, X. Zhu, Z. Zhou, S.-W. Zhang, D. Yang, B. Zhao, Y.-P. Zhang, J. Deng, Y. Cheng, Y.-X. Zheng, S.-Q. Zang, H. Kuang, P. Duan, M. Yuan, C.-F. Chen, Y. S. Zhao, Y.-W. Zhong, B. Z. Tang and M. Liu, *Sci. China:Chem.*, 2021, **64**, 2060–2104.
28 J.-F. Chen, Q.-X. Gao, H. Yao, B. Shi, Y.-M. Zhang, T.-B. Wei and Q. Lin, *Chem. Commun.*, 2024, **60**, 6728–6740.
29 K. Maeda, M. Nozaki, K. Hashimoto, K. Shimomura, D. Hirose, T. Nishimura, G. Watanabe and E. Yashima, *J. Am. Chem. Soc.*, 2020, **142**, 7668–7682.
30 H. Yan, Y. He, D. Wang, T. Han and B. Z. Tang, *Aggregate*, 2023, **4**, e331.
31 T. Ikai, S. Shimizu, S. Awata and K.-i. Shinohara, *Macromolecules*, 2018, **51**, 2328–2334.
32 Y. Zhang, H. Li, Z. Geng, W.-H. Zheng, Y. Quan and Y. Cheng, *ACS Nano*, 2022, **16**, 3173–3181.
33 Y. He, J. Zhang, C. Ma, J. Liu, J. Guo, T. Han, R. Hu, B. S. Li and B. Z. Tang, *Aggregate*, 2024, e642.
34 S. Du, Y. Jiang, H. Jiang, L. Zhang and M. Liu, *Angew. Chem., Int. Ed.*, 2024, **63**, e202316863.
35 Y. Chen, Y. Zhang, H. Li, Y. Li, W. Zheng, Y. Quan and Y. Cheng, *Adv. Mater.*, 2022, **34**, 2202309.
36 Q. Guo, M. Zhang, Z. Tong, S. Zhao, Y. Zhou, Y. Wang, S. Jin, J. Zhang, H.-B. Yao, M. Zhu and T. Zhuang, *J. Am. Chem. Soc.*, 2023, **145**, 4246–4253.
37 Y. Shi, J. Han, C. Li, T. Zhao, X. Jin and P. Duan, *Nat. Commun.*, 2023, **14**, 6123.
38 M. Pan, R. Zhao, B. Zhao and J. Deng, *Macromolecules*, 2021, **54**, 5043–5052.
39 Y. Jiang, W. Su, G. Li, Y. Fu, Z. Li, M. Qin and Z. Yuan, *Chem. Eng. J.*, 2022, **430**, 132780.
40 Z. Li, C. Zhao, X. Lin, G. Ouyang and M. Liu, *ACS Appl. Mater. Interfaces*, 2023, **15**, 31077–31086.

© 2025 The Author(s). Published by the Royal Society of Chemistry

Open Access Article. Published on 18 February 2025. Downloaded on 2/21/2026 7:16:46 PM. This article is licensed under a Creative Commons Attribution-NonCommercial 3.0 Unported Licence.

41 L. Xing, G. Li, Y. Sun, X. Wang, Z. Yuan, Y. Fu and M. Qin, *Carbohydr. Polym.*, 2023, **313**, 120856.
42 L. Wei, S. Guo, B. Zhang, B. Jiang, Y. Wang, Z. Liu, Y. Xu, Y. Gong, Y. Liu and W. Z. Yuan, *Adv. Funct. Mater.*, 2024, **34**, 2409681.
43 Y. Wang, Q. Sun, L. Yue, J. Ma, S. Yuan, D. Liu, H. Zhang, S. Xue and W. Yang, *Adv. Opt. Mater.*, 2021, **9**, 2101075.
44 K. Wang, R. Hu, J. Wang, J. Zhang, J. Liu, L. Zhou, L. Zhou and B. Li, *ACS Mater. Lett.*, 2022, **4**, 2337–2344.
45 L. Wan, K. Wang, J. Liu, X. Yang and B. Li, *Adv. Funct. Mater.*, 2024, 2413609.
46 S. Sona, D. Hirose, Y. Kurihara and K. Maeda, *J. Mater. Chem. C*, 2023, **11**, 1271–1277.
47 A. Ikenaga, Y. Akiyama, T. Ishiyama, M. Gon, K. Tanaka, Y. Chujo and K. Isoda, *ACS Appl. Mater. Interfaces*, 2021, **13**, 47127–47133.
48 X. Lin, G. Ouyang and M. Liu, *ACS Appl. Mater. Interfaces*, 2023, **15**, 19741–19749.
49 W.-T. Xu, X. Li, P. Wu, W.-J. Li, Y. Wang, X.-Q. Xu, X.-Q. Wang, J. Chen, H.-B. Yang and W. Wang, *Angew. Chem., Int. Ed.*, 2024, **63**, e202319502.
50 Q. Xia, W. Xie, T. He, H. Zhang, Z. Zhao, G. Huang, S. Li Bing and Z. Tang Ben, *CCS Chem.*, 2022, **5**, 1663–1673.
51 L. Ai, H. Wang, B. Wang, S. Liu, H. Song and S. Lu, *Adv. Mater.*, 2024, **36**, 2410094.
52 J. Yin, L. Xu, X. Han, L. Zhou, C. Li and Z.-Q. Wu, *Polym. Chem.*, 2017, **8**, 545–556.
53 B. Zhao, K. Pan and J. Deng, *Macromolecules*, 2019, **52**, 376–384.
54 X. Gao, J. Wang, K. Yang, B. Zhao and J. Deng, *Chem. Mater.*, 2022, **34**, 6116–6128.
55 B. Zhao, H. Yu, K. Pan, Z. a. Tan and J. Deng, *ACS Nano*, 2020, **14**, 3208–3218.
56 H. Yang, S. Ma, B. Zhao and J. Deng, *ACS Appl. Mater. Interfaces*, 2023, **15**, 13668–13677.

© 2025 The Author(s). Published by the Royal Society of Chemistry